Remote Sensing in Ecology and Conservation
Open Access
ZSL LET'S WORK FOR WILDLIFE

ORIGINAL RESEARCH

Drone-based thermal remote sensing provides an effective new tool for monitoring the abundance of roosting fruit bats

Eliane D. McCarthy[1], John M. Martin[2], Matthias M. Boer[1] & Justin A. Welbergen[1]

[1]The Hawkesbury Institute for the Environment, Western Sydney University, Richmond NSW, 2753, Australia
[2]Institute of Science and Learning, Taronga Conservation Society Australia, Bradleys Head Road, Mosman NSW, 2088, Australia

Keywords
Computer vision, flying-fox, infrared, machine learning, orthomosaic, remotely piloted aircraft

Correspondence
Eliane D. McCarthy, The Hawkesbury Institute for the Environment, Western Sydney University, Richmond, NSW 2753, Australia. Tel: +61 2 4570 1125; Fax: +61 2 4570 1103; E-mail: eliane.d.mccarthy@gmail.com

Editor: Ned Horning
Associate Editor: Margarita Mulero-Pazmany

Received: 30 October 2020; Revised: 19 January 2021; Accepted: 26 February 2021

doi: 10.1002/rse2.202

Remote Sensing in Ecology and Conservation 2021;**7** (3):461–474

Abstract

Accurate and precise monitoring of species abundance is essential for determining population trends and responses to environmental change. However, traditional population survey methods can be unreliable and labour-intensive, which complicates the effective conservation and management of many threatened species. We developed a method of using drone-acquired thermal orthomosaics to monitor the abundance of grey-headed flying-foxes (*Pteropus poliocephalus*) within tree roosts, an IUCN Red Listed species of bat. We assessed the accuracy and precision of this new method and evaluated the performance of four semi-automated methods for counting flying-foxes in thermal orthomosaics, including machine learning and Computer Vision (CV) methods. We found a high concordance between the number of flying-foxes manually counted in drone-acquired thermal imagery and the true abundance of flying-foxes in single roost trees, as obtained from direct on-ground observation. This indicated that the number of flying-foxes observed in thermal imagery accurately reflected the true abundance of flying-foxes. In addition, for thermal orthomosaics of whole roost sites, the number of flying-foxes manually counted was highly repeatable between the same-day drone surveys and human counters, indicating that this method produced highly precise abundance estimates independent of the identity/experience of human counters. Finally, the number of flying-foxes manually counted in drone-acquired thermal orthomosaics was highly concordant with the counts derived from CV and machine learning-enabled classification techniques. This indicated that accurate and precise measures of colony abundance can be obtained semi-automatically, thus greatly reducing the amount of human effort involved for obtaining abundance estimates. Our method is thus valuable for reliably monitoring the abundance of individuals in flying-fox roosts and will aid in the conservation and management of this globally threatened group of flying-mammals, as well as other homeothermic arboreal-roosting species.

Introduction

Quantifying the size of animal populations is a fundamental activity in conservation biology (Gibbs, 2000; Marsh & Trenham, 2008). Population surveys provide information about the population status of a species, while monitoring populations over time can elucidate population trends (Woinarski, 2018) and determine the effectiveness of management practices (Reddiex et al., 2006). The validity of population surveys may be biased by several factors (Seber, 1986) including changes in population size (Manning et al., 1995), accessibility (Reddy & Dávalos, 2003; Wagner, 1981) and observer variability (Erwin, 1982). Critically, inaccurate and imprecise population survey methods may lead to ill-informed conclusions about species' status and trends (Goldsmith, 1991; Guschanski et al., 2009; Margalida et al., 2011).

Recent technological advances have made remotely piloted aircraft systems (hereafter 'drones') more affordable and available for use as a remote sensing instrument (Jiménez López and Mulero-Pázmány, 2019). Drones are used increasingly as tools for studying wildlife and tend to be quieter, more manoeuvrable, and cause less disturbance than traditional, piloted aircraft (Christie et al., 2016). Advances in drone technology have been paralleled by improvements in sensor resolution, including thermal imaging devices (Wich & Koh, 2018). Drones equipped with thermal sensors are being used for an increasing diversity of applications in wildlife conservation and management. Recent examples include: automatically identifying and ageing populations of grey seals (*Halichoerus grypus*) (Seymour et al., 2017); detecting and counting arboreal mammals (Corcoran et al., 2019; Kays et al., 2019; Spaan et al., 2019); and surveying common hippopotamus (*Hippopotamus amphibius*) (Lhoest et al., 2015).

Maps derived from Structure from Motion photogrammetry have allowed researchers to create high resolution orthomosaics, and quantify a diverse range of species spread over large spatial scales (Bycroft et al., 2019; Francis et al., 2020; Old et al., 2019). However, manually counting animals in remotely sensed imagery is time consuming and often subject to human error (Erwin, 1982; Harris & Lloyd, 1977). Furthermore, as the volume and availability of aerial imagery increases, there is a real benefit to developing automated methods for image analysis (Terletzky & Ramsey, 2016). Machine learning-enabled classification techniques are increasingly being applied in ecology, including species population monitoring (Dell et al., 2014; Tabak et al., 2019; Valletta et al., 2017; Yang et al., 2015). Object-based image analysis (OBIA) is a machine learning technique based upon segmentation of an image into groups of spatially and spectrally connected pixels, or image objects. OBIA machine learning classification workflows have been used in ecological studies to identify, classify and quantify populations of coral (Phinn et al., 2012), vegetation (Dronova et al., 2012) and marine birds (Groom et al., 2013). By contrast, Computer Vision (CV) is a branch of computer science where classification is user-driven. CV allows the user to define rules and infer information about an image based on pixel characteristics, such as intensity, shape and texture (Weinstein, 2018). CV has applications in automated species identification, counting, tracking (Dell et al., 2014) and examination of morphological characteristics (Weinstein, 2018).

Flying-foxes or Old World fruit bats, of the family Pteropodidae, are largely understudied (International Union for Conservation of Nature & Natural Resources, 2020) and difficult to monitor due to their high mobility, expansive distribution and the inaccessibility of roosting sites (van Toor et al., 2019; Welbergen et al., 2020). They are distributed throughout Africa, southeast Asia, Australia and the Indo-Pacific, where they are considered ecosystem engineers, performing pollination and seed dispersal (Cox et al., 1991; Fujita & Tuttle, 1991). Pteropodidae are threatened throughout their range by habitat loss (Mohd-Azlan et al., 2001), climate change (Welbergen et al., 2008) and overhunting (Brooke & Tschapka, 2002). According to the IUCN Red List, the populations of 82 species of Pteropodids are decreasing, while for a further 59 species their population status is unknown (International Union for Conservation of Nature & Natural Resources, 2020). Effective monitoring of these species is needed globally for more reliable conservation management.

In mainland Australia, there are four *Pteropus* species, of which the grey-headed flying-fox (*Pteropus poliocephalus*) is listed as Vulnerable and the spectacled flying-fox (*Pteropus conspicillatus*) is listed as Endangered (Commonwealth of Australia Department of Environment & Energy, 2019). During the day, these species are found in roosts (or 'camps') where they form colonies of a few hundred to many thousands of individuals in the canopies of trees, in natural, agricultural, and urban bushland areas (Eby et al., 1999; Markus & Hall, 2004; Tait et al., 2014). Presently in Australia, the number of individuals that comprise a colony at a roost (defined here as 'colony size') is estimated by ground counts (also known as 'static counts'), where people count the number of individuals present during the day, and fly-out counts, where people count individuals as they emerge from the roost in streams at dusk (Forsyth et al., 2006; Westcott & McKeown, 2004). Accurate ground counts require counters to walk through a flying-fox roost, which can be impractical with dense vegetation and can also cause a high degree of disturbance, while fly-out counts have been shown to be inaccurate and imprecise (Forsyth et al., 2006; Westcott & McKeown, 2004). The development of more accurate monitoring practices for assessing flying-fox colony size would enhance the evidence base for effective conservation and management of these species (Westcott et al., 2015).

Here, we describe a drone-based methodology for producing thermal orthomosaics of flying-fox colonies and quantifying the local abundance (number of individuals present in the colony) of flying-foxes. We assess the accuracy of counts from drone-acquired thermal imagery by comparing them to the true abundance from exhaustive ground counts, in 15 single trees across three colonies throughout the Greater Sydney region, New South Wales. We then determine the precision of counts derived from the thermal orthomosaic method by examining the variability of flying-fox colony size counts between counters

and between multiple orthomosaics captured on the same day. Following this, four semi-automated approaches, CV and OBIA machine learning involving Maximum Likelihood, Random Forest and Support Vector Machines algorithms, are used to quantify the number of individuals in a series of orthomosaics of flying-fox colonies throughout the Greater Sydney region to determine the most reliable approach for semi-automated counting of flying-foxes in their roosts.

Materials and Methods

Drone and sensor

A DJI Inspire 1 Version 2.0 drone equipped with Zenmuse XT 19 mm radiometric thermal camera, with a combined mass of 3.2 kg, was used to obtain thermal imagery of flying-fox colonies. The FLIR longwave infrared thermal sensor in the Zenmuse XT has a sensitivity of 50 mK @nf/1.0 at a resolution of 640 × 520 pixels.

The Drone Observing tool (Burke et al., 2019) was used to determine the optimal flight height for thermal image acquisition (nadir) with an approximate resolution of 0.02 m per pixel, corresponding to *c.* 5 × 5 pure pixels per flying-fox. Flying-foxes appeared as circular objects in aerial thermal imagery, with an estimated diameter of *c.* 0.10 m (based on measurements from Meade et al., 2019). Accounting for mean estimated height of local roost vegetation (27.3 ± 0.6 m) (Timmiss, 2021) and the size of roosting flying-foxes, the required flight height was determined to be 23 m above roosting flying-foxes, and hence the drone was set to fly at 50 m above ground level (AGL) for all surveys (Eisenbeiss & Sauerbier, 2011).

Thermal orthomosaic construction

Thermal orthomosaics were obtained from drone surveys conducted when wind speed was below 10 km h^{-1}. All flights were programmed in flight planning application Pix4Dcapture 4.9.0 (Pix4D, 2017). Take-off and landing were autonomous, and images were taken while the drone was in cruising mode, flying at 2 m s^{-1} in a lawnmower pattern, with 90% front and side overlap. Collecting informative orthomosaic imagery for this study relied on flying-fox external body temperature being sufficiently different to ambient background temperature (Figure 1). Therefore, all drone surveys were conducted during the cooler part of the day (commencing 66–130 min after sunrise) to maximize the difference between ambient temperature and animal external body temperature (see Burke et al., 2019). Roost surveys were conducted between September 2019 and March 2020 (throughout Spring, Summer and Autumn) where ambient temperature ranged from 5.0 to 22.6°C, with a mean temperature of 18.3°C, recorded concurrently at the nearest weather station (Bureau of Meteorology, 2020).

Following drone surveys, all survey images were saved as radiometric JPEGs, with embedded EXIF data providing latitude, longitude, and altitude. Agisoft Metashape Professional Version 1.5 was used to generate orthomosaics (Supplementary Material 1.1) (LLC Agisoft, 2019).

Accuracy assessment

To determine the accuracy of counting flying-foxes in drone-acquired thermal imagery, we assessed the concordance between the true abundance based on ground counts of flying-foxes in single trees to counts obtained by drone-acquired thermal imagery. In February 2020, direct visual counts of flying-foxes roosting in a single tree were conducted at Camellia Gardens at 1.5–2 h after sunrise, in air temperature of 19.0°C, Centennial Park at 2.5–3 h after sunrise, in air temperature of 23.9°C, and Macquarie Fields at 7.5–8 h after sunrise, in air temperature of 24.4°C (concurrent air temperatures were obtained from the nearest weather station (Bureau of Meteorology, 2020).

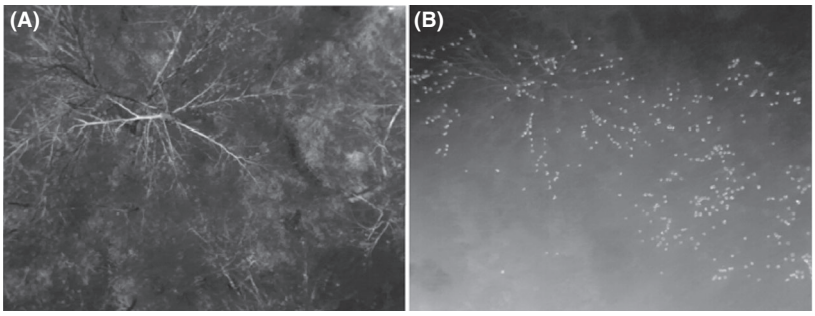

Figure 1. Drone-acquired thermal image of flying-fox colony at Emu Plains, New South Wales, taken when air temperature was (A) 29°C and (B) 10°C. Flying-foxes in (B) are bright and easily distinguishable from dark (cooler) background, while in (A), there is markedly less spectral contrast between the flying-foxes and the vegetation.

The author EDM exhaustively counted the exact number of flying-foxes present in five trees at the three roosts while standing directly underneath each tree. Upon completion of EDM's count at a focal tree, a thermal image of the tree was taken by the drone positioned at 50 m AGL with its the camera aimed in nadir direction. Following image capture, the number of thermal signatures of flying-foxes in each target tree was manually counted in the image with the aid of the multi-point tool in Fiji 1.8.0_172 by author EDM (Schindelin et al., 2012) (Supplementary Material 1.2).

Precision assessment

To determine the precision of manual counts derived from drone-acquired thermal orthomosaics, we compared manual point counts derived from repeated surveys, the number of flying-foxes in each orthomosaic was counted manually using the multi-point tool in Fiji 1.8.0_172 (Schindelin et al., 2012). Orthomosaics were generated from repeated surveys on the same day at four roosts (Supplementary Material 1.3, Supplementary Material 2). For 10 of 11 orthomosaics, resolution was constant to within ± 0.12 cm^2/pixel for orthomosaics captured at the same roost (Supplementary Material 1.3). However, for the three orthomosaics generated for the Kareela roost, the resolution of 'Kareela 3' was *c.* 1.8 cm^2/pixel lower than the resolution of 'Kareela 1' and 'Kareela 2'.

To determine the extent of between-counter variability in manual point counts, the set of three orthomosaics for the Kareela roost was manually counted by author EDM and four additional human counters. The additional counters were selected on the basis that they were familiar with the species and had visited a flying-fox colony. Each counter was sent an email outlining the purpose of the task, the three orthomosaics (Supplementary Material 2), and a set of instructions for completing the task (Supplementary Material 1.4). All orthomosaics were randomized prior to sharing with counters, and the counters worked independently from each other. The counters reported that it took up to 1 h to conduct a manual point count of an orthomosaic (for an average of 1983 flying-foxes counted over an area of *c.* 2654 m^2) (Supplementary Material 1.3).

Performance of semi-automated methods

We compared the counts obtained by the four semi-automated approaches to those from the manual point counts of a series of 13 thermal orthomosaics of eight flying-fox colonies throughout the Greater Sydney region. Two orthomosaics were generated for five roosts and one orthomosaic was generated for three roosts (Supplementary Material 1.5). The average resolution of the colony orthomosaics varied from 2.53 to 8.24 cm^2/pixel, with an average orthomosaic resolution of 4.24 cm^2/pixel. Lower orthomosaic resolutions resulted because photogrammetry software was unable to successfully align some survey images in the orthomosaic (Yang & Lee, 2019). This may have been due to environmental factors such as wind-induced movement of foliage in the image between successive images, or to changes in solar radiation. The colony area of each orthomosaic was measured by tracing around the spatial extent of the colony in ArcGIS Pro, and varied between 1451 m^2 at Camellia Gardens to 21 112 m^2 at Centennial Park.

For each thermal orthomosaic, author EDM conducted a manual point count of the number of flying-foxes. Manual point counts of flying-foxes in the orthomosaics varied from 1126 to 12 131 individuals (Supplementary Material 1.5), and these served as the baseline for comparisons with counts obtained from semi-automated methods.

Following the manual point counts, the number of flying-foxes in the same orthomosaics were estimated using four semi-automated approaches: CV and OBIA machine learning (involving Maximum Likelihood, Random Forest and Support Vector Machines algorithms) (thermal orthomosaics and classified products are viewable in Supplementary Material 2).

CV method

The 13 thermal orthomosaics were classified using CV-driven image analysis, adapted from cell counting methods (Drury et al., 2011; Grishagin, 2015), and implemented in Fiji 1.8.0_172 (Schindelin et al., 2012). The optimum functions and parameters for this process were determined by systematically adding one function or varying one parameter at a time while keeping all others constant. The classification proceeded according to the steps outlined in Figure 2. For the final step, 'Analyse Particles', the size range was set to 10–300 pixels and the circularity to 0.3–100, with 'Include Holes' enabled. A region of interest was generated for each segment of pixels representing a flying-fox. The macro for this process is given in Supplementary Material 1.6.

OBIA method

The 13 orthomosaics were classified using ArcGIS Pro 2.5.0 (Environmental Systems Research Institute, 2020) through an OBIA supervised classification machine learning approach. A 5% clip stretch was applied to increase the contrast between flying-foxes and the background. A 'segment mean shift' approach was applied to each orthomosaic (Comaniciu & Meer, 2002) where areas with

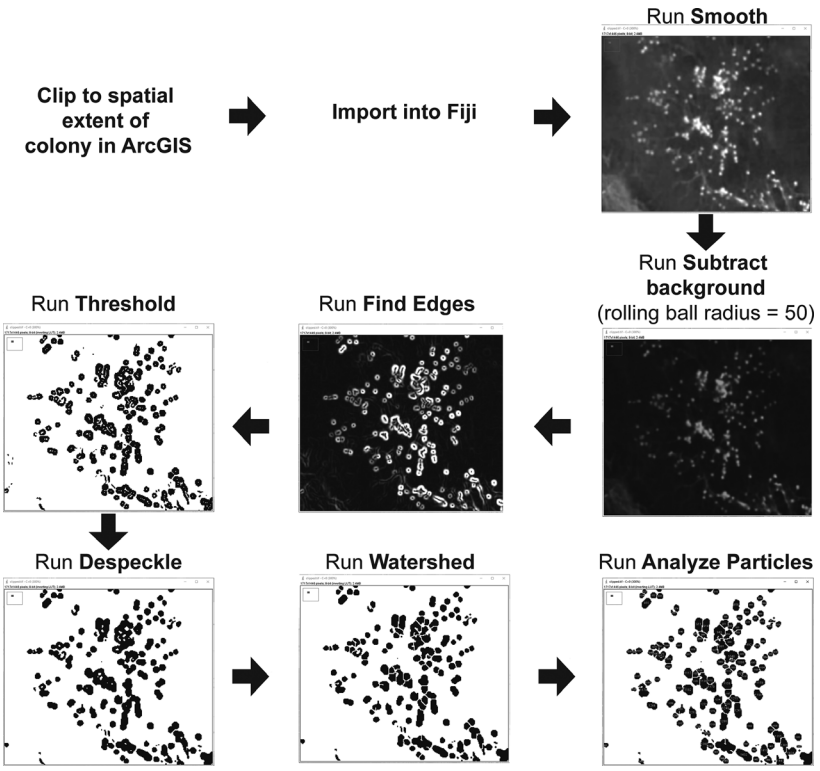

Figure 2. Flowchart outlining the steps taken to generate a semi-automated colony size estimate of the flying-fox colony at Yarramundi through Computer Vision – implemented in Fiji 1.8.0_172 (Schindelin et al., 2012). Images depict the classification process for a small area of the colony.

homogenous intensity were grouped together (spectral detail = 15, spatial detail = 15.5). The minimum segment size was set to three pixels, to ensure that the smaller or partially covered flying-foxes were represented in the segmented product. Then, training samples were generated for the classification scheme that was made up of flying-fox and background classes. For each orthomosaic, 100 training samples were generated for each class using the segment picker and freehand selection tools. Next, each orthomosaic was classified using Random Forest, Maximum Likelihood and Support Vector Machines classifiers (parameters provided in Supplementary Material 1.7). Each classified orthomosaic was imported into Fiji 1.8.0_172 (Schindelin et al., 2012) and the 'Watershed' function was applied to separate individuals roosting close together in imagery. Then, the 'Analyze Particles' tool was used to quantify the number of segments classified as flying-foxes (this workflow is illustrated in Supplementary Material 1.8).

Pixel-based accuracy assessment

Pixel-based accuracy assessments were conducted for all classified orthomosaics generated using the four semi-automated counting approaches. For each classified orthomosaic, the classification accuracy of one-hundred pixels classified as 'flying-fox', and one-hundred pixels classified as 'background' was determined by visual comparison with the original thermal orthomosaic (pixels were selected through random stratified sampling). Results were used to generate a confusion matrix for each classified orthomosaic (Supplementary Material 1.9). From this, classification accuracy (%) was calculated.

Statistical analyses

All statistical analyses were two-tailed, employed an α value of 0.05 and were conducted in R version 3.6.3 (R Core Team, 2018). General linear mixed models (GLMMs) were constructed using the *nlme* package (Pinheiro et al., 2016). All models had a Gaussian distribution and were fitted with an identity link function. To analyse the relationship between thermal image point count and true abundance, derived from ground count for single trees, we constructed a GLMM with thermal image point count as the response variable, ground count as the fixed effect and roost ID as a random effect. The effect of the response variable was tested through a likelihood ratio test (ANOVA). To determine the concordance between ground counts and thermal image point counts of a single tree, we calculated Lin's concordance correlation

coefficient (ρc) (Lawrence & Lin, 1989) using the package *DescTools* (Signorell, 2016).

To test the effect of roost ID on the difference between thermal image counts and ground counts, and thus the effect of roost ID on thermal image point count accuracy, we ran an ANOVA, with 'thermal image point count – ground count' as the response variable, and roost ID as the independent variable. Here, we used a Tukey's test to test for between-level effects post hoc.

To determine the extent of variability between manual point counts of flying-foxes in thermal orthomosaics from repeated surveys of colonies on the same day, and thus the precision of manual point counts, we calculated relative standard error (RSE) for all counts of the orthomosaics, grouped by roost.

To test whether there was a significant difference between the counts obtained from the Kareela roost orthomosaics by different counters, a two-way ANOVA was run, and a Tukey's test was used to test for between-level effects post-hoc. To test for homogeneity of variance between the counts grouped by counter and by image, two Levene's tests were run using the package *car* (Fox et al., 2012).

To determine the relationship between flying-fox colony abundance estimates, generated using the semi-automated counting methods and manual point counts, four GLMMs were fitted using manual point count as the response variable in the package *nlme* (Pinheiro et al., 2016). For each GLMM, counts obtained through each of the semi-automated methods, including CV, Support Vector Machines, Maximum Likelihood and Random Forest, were fitted as a fixed effect. Bayesian Information Criterion (BIC) values for each of the four GLMMs were compared. For all semi-automated counting methods, models accounting for the effect of roost as a random effect failed to improve fit, based on BIC, and roost was excluded from the final models.

To determine the concordance between the counts obtained from each of the semi-automated counting methods and manual point counts, Lin's concordance correlation coefficient (ρc) (Lawrence & Lin, 1989) was calculated for each semi-automated method using the package *DescTools* (Signorell, 2016).

A GLMM was constructed to determine the relationship between the accuracy of each classified orthomosaic (through pixel-based accuracy assessments) and the difference between the counts generated using the semi-automated methods and manual point counts. The GLMM was fitted with accuracy as the response variable; absolute value percent difference between the semi-automated and manual point count (%), and semi-automated method type as the fixed effects; and roost as a random effect. For this GLMM, the significance of the fixed effects was tested through likelihood ratio tests (ANOVAs), and Tukey's test was used to test for between level effects post-hoc. In this analysis, the Maximum Likelihood classified product for the Campbelltown orthomosaic was excluded as an outlier as the manual point count differed 268% from the Maximum Likelihood classified count.

Animal ethics statement

This research was approved by Western Sydney University Animal Research Authority no. A12217 and NPWS scientific licence SL102047.

Results

Accuracy assessment

For single trees, point counts derived from drone-acquired thermal images were strongly positively related to true abundance as derived from ground counts (GLMM: $F_{1,11} = 71.860$, $P < 0.001$, marginal $R^2 = 0.88$; Figure 3). Furthermore, counts derived from thermal drone imagery had a high level of concordance with ground counts (ρc = 0.89, 95% CI 0.73–0.96). Roost ID had a significant effect on the accuracy of thermal image point counts (ANOVA: $F_{2,12} = 9.06$, $P = 0.004$). The accuracy of thermal image point counts was significantly lower for the Macquarie Fields roost compared to the Centennial Park roost (Tukey's test: $P = 0.003$).

Precision assessment

The RSE between manual point counts of flying-foxes visible in orthomosaics for the three repeated surveys varied from 0.92% for the three Campbelltown orthomosaics, to 6.91% for the three Kareela orthomosaics, with an average of 2.22% for all orthomosaics, excluding the lower resolution Kareela 3 orthomosaic (Supplementary Material 1.3).

There was no significant effect of human counter on the number of flying-foxes counted for three Kareela orthomosaics (ANOVA: $F_{4,9} = 1.06$, $P = 0.433$; Supplementary Material 1.10A). However, counts varied significantly between the three orthomosaics of the colony at Kareela (ANOVA: $F_{1,9} = 23.53$, $P < 0.001$), with the counts of 'Kareela 3' being significantly different from 'Kareela 1' and 'Kareela 2' (Tukey's test: $P = 0.001$ and $P < 0.001$, respectively) (Supplementary Material 1.10B).

Semi-automated counts

Counts of thermal orthomosaics derived from semi-automated methods correlated strongly with those derived from manual point counts (Figure 4; Supplementary Material 1.5). The Random Forest classification semi-

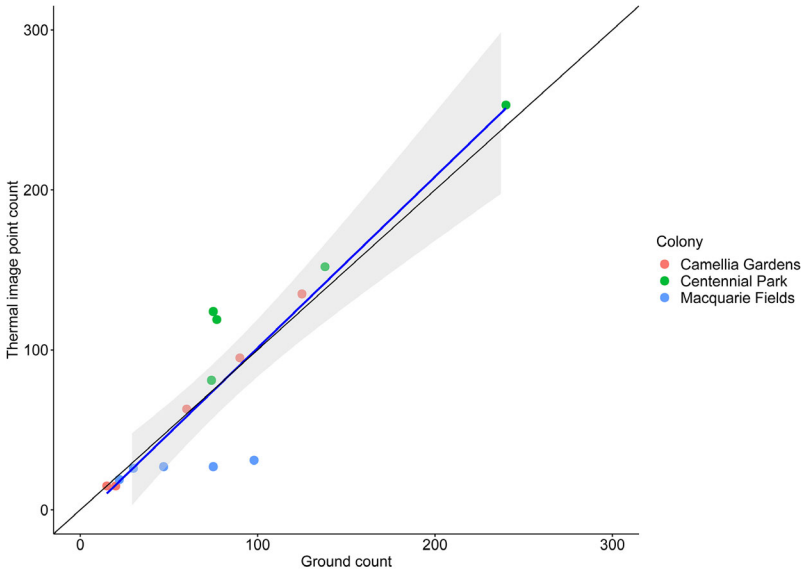

Figure 3. Relationship between ground counts and counts obtained from thermal images for a single tree. Grey shaded area indicates ± SE (standard error).

automated method had the strongest positive relationship with manual point counts (GLMM: BIC = 56.09). The subsequent rank of semi-automated methods was: CV (GLMM: BIC = 57.12), Support Vector Machines (GLMM: BIC = 58.06) and Maximum Likelihood (GLMM: BIC = 67.15), compared to a BIC of 70.78 for the model run without the fixed effect.

Counts resulting from the CV method had the highest concordance with manual point counts (ρc = 0.83, 95% CI 0.57–0.94; Figure 5), followed by Support Vector Machines (ρc = 0.81, 95% CI = 0.53–0.93), Maximum Likelihood (ρc = 0.70, 95% CI = 0.28–0.89) and Random Forest (ρc = 0.70, 95% CI = 0.28–0.89).

From pixel-based accuracy assessments (Supplementary Materials 1.9 and 1.11), the accuracy of semi-automatically classified orthomosaics for all four classification methods, ranged from 66.5% to 97.5%, with an average accuracy of 84.0%. There was no significant relationship between accuracy and the absolute value percent difference between the count obtained through each semi-automated method and manual point count (GLMM: $F_{1,40} = 0.15$, $P = 0.705$). Accuracy differed significantly between the semi-automated methods (GLMM: $F3,40 = 6.66$, $P < 0.001$). There was a significant difference in accuracy between the Maximum Likelihood and Support Vector Machines methods (Tukey's test: $P = 0.008$).

Discussion

We demonstrated that drone-acquired thermal imagery can be used to accurately and precisely quantify the abundance of flying-foxes in a roost. In addition, we show that semi-automatic CV and OBIA workflows generate results that are comparable to manual point counts of thermal orthomosaics of colonies, providing an efficient alternative to manually assessing the number of flying-foxes in thermal orthomosaics. Drones equipped with thermal cameras have previously been recommended as a powerful tool for the remote detection of animals (Burke et al., 2019) and have been used to help determine population sizes of several species (Dunstan et al., 2020; Lhoest et al., 2015; Seymour et al., 2017). Our results add to this field of research, demonstrating that drone-acquired thermal remote sensing can be used as an effective tool for monitoring colonies of the Vulnerable grey-headed flying-fox. Implementing this method to improve our understanding of the globally threatened *Pteropus* species, including data-deficient species, would greatly enhance our ability to inform conservation planning for this ecologically important genus throughout Africa, southeast Asia, Australia and the Indo-Pacific.

It was critical for us to assess the ability of users to detect roosting flying-foxes in drone-acquired thermal imagery. Counts of the number of flying-foxes in single trees derived from drone-acquired thermal imagery were concordant, and strongly and linearly related to, the true abundance of flying-foxes in those trees, indicating that counts from drone-acquired thermal imagery was accurate. However, for the Macquarie Fields roost, some flying-foxes were not visible in thermal imagery, and consequently those counts were lower than ground counts (Figure 3). This may have been due to higher ambient

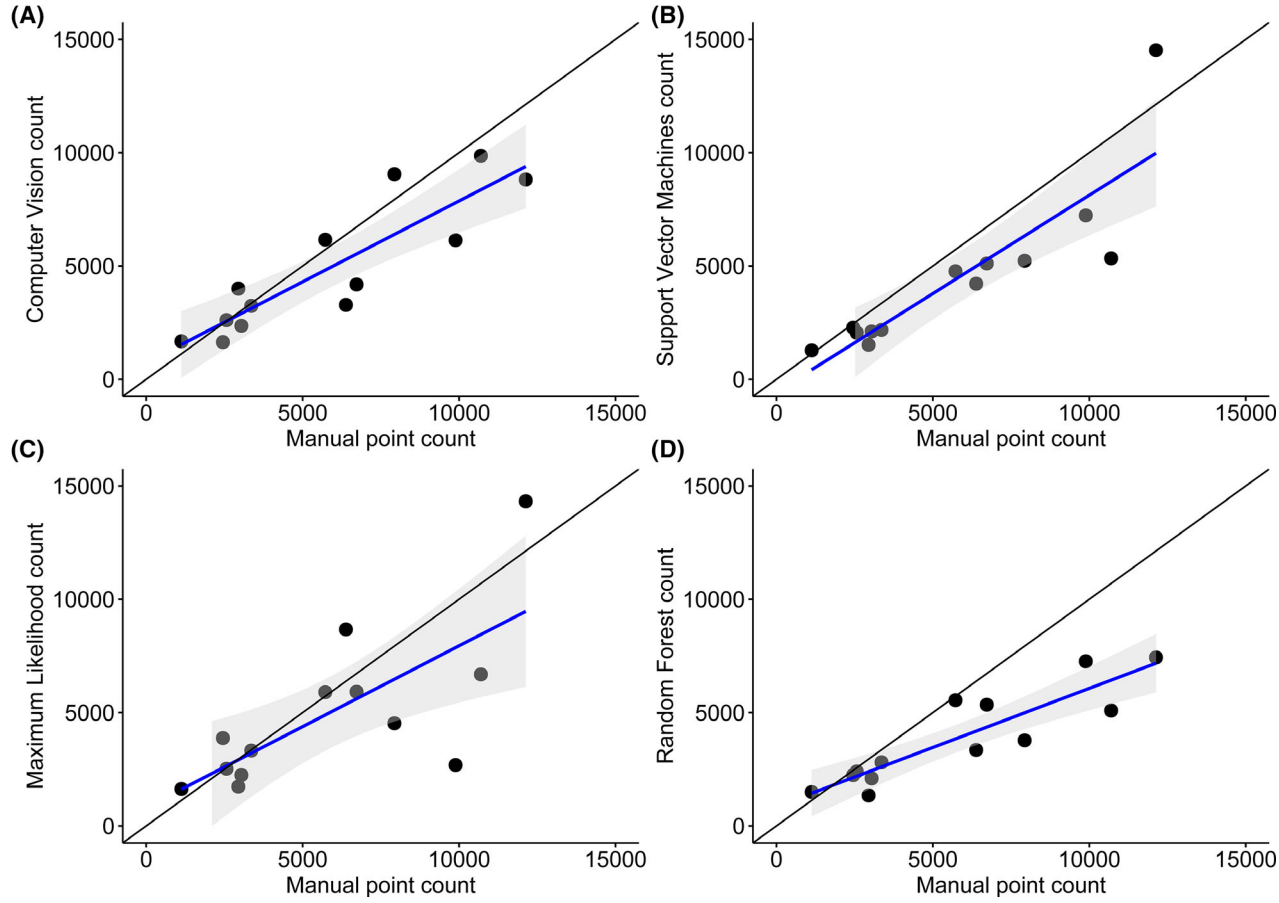

Figure 4. Relationship between manual point counts by author EDM and counts obtained through each of the semi-automated counting methods: (A) Computer Vision, (B) Support Vector Machines, (C) Maximum Likelihood and (D) Random Forest. Grey shaded area indicates ± 95 CI (confidence interval). Blue lines show fits from linear models. Black lines are lines of equality.

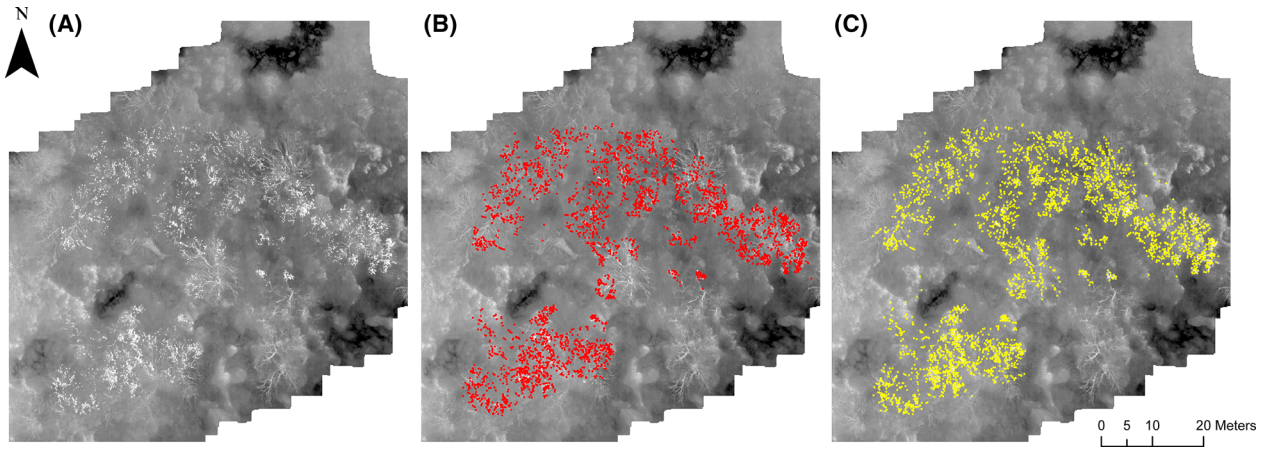

Figure 5. (A) Complete thermal orthomosaic of the flying-fox colony at Yarramundi on the 4th of September 2019. (B) Orthomosaic with red points giving locations of flying-foxes manually counted by author EDM. (C) Orthomosaic with yellow points of flying-foxes detected using the Computer Vision workflow, which delivered counts most concordant with manual point counts (Figure 4A; Supplementary Material 1.5). Points represent locations of image segments classified as flying-foxes.

temperature and higher sun elevation at Macquarie Fields, as it was later in the day, warming the vegetation (see Burke et al., 2019; Mulero-Pázmány et al., 2014), making flying-foxes thermal signature less distinguishable from the background environment. Ambient temperature is understood to affect the visibility of animals in thermal imagery (Cilulko et al., 2013; Kays et al., 2019; Spaan et al., 2019), and hence we recommend that thermal imagery surveys of flying-fox colonies should be undertaken early in the day, to avoid underestimating the number of individuals present.

There was little variation between manual point counts of thermal orthomosaics from repeated same-day surveys at four roosts, indicating that thermal orthomosaics can yield precise estimates of flying-fox abundance. Of the four colonies, the variation between repeated counts was highest for the Kareela colony, with the 'Kareela 3' orthomosaic yielding significantly lower flying-fox abundance estimates than the other two orthomosaics from earlier that day. This may be explained by the fact that the resolution of the 'Kareela 3' orthomosaic was substantially lower than the colony's other two orthomosaics (Supplementary Material 1.3). Low orthomosaic resolution has previously been noted as a potential source of error in visual spectrum imagery (Bycroft et al., 2019). Formal assessments of the effects of orthomosaic resolution on flying-fox abundance estimates at a colony would further increase the precision and accuracy of this method. Nonetheless, users should ensure that orthomosaics are of a sufficiently high resolution (ideally 2–3 cm^2/pixel) to represent each flying-fox as 3–5 pixels (Meade et al., 2019).

No significant effect of human counter was found on manual point counts of flying-fox colonies derived from drone-acquired thermal orthomosaics, suggesting that manually counting flying-foxes in drone-acquired thermal orthomosaics does not require specialized skills. Between-observer variability is often cited as a source of error in animal population surveys that employ both ground-based and aerial surveillance techniques (Bowler et al., 2020; Stapleton et al., 2014). Results from ground-based animal detection surveys have been shown to depend on observer experience, when spotting koalas (*Phascolarctos cinereus*) (Hanger et al., 2017) as well as for estimating flying-fox colony size from fly-out counts (Forsyth et al., 2006). Contrastingly, counts of rafting canvasbacks (*Aythya valisiner*) from black-and-white aerial photographs did not vary significantly between counters with different levels of training and experience (Erwin, 1982). We suggest that manual point counts of thermal orthomosaics of flying-fox colonies may be reliably conducted by any individual, provided they are familiar with the counting software and the appearance of flying-foxes in drone-acquired thermal imagery. This will thus be valuable for small organisations who may not have knowledge of semi-automated counting techniques.

Flying-fox colony size estimates derived from the semi-automated methods matched those from the manual point counts well, indicating that semi-automated methods provide an efficient alternative to the time-consuming process of manually assessing the number of flying-foxes in thermal orthomosaics. Flying-fox colony size estimates derived from the CV workflow had the highest concordance with manual point counts (Figure 5) and the second highest correlation with manual point counts. CV techniques are commonly used in the life sciences to characterize and quantify microorganisms under a microscope (Grishagin, 2015) but also have many applications in ecology (Seymour et al., 2017; Weinstein, 2018). In most ecological studies the target organisms are highly distinguishable against a homogenous background; however, in this study, the background was often heterogenous and always three-dimensional, and we had to subtract the background and manually threshold each image. Critically, when thresholding a thermal orthomosaic, the operator aims to visually optimize the brightness in the image to the point where the contrast between individual flying-foxes and surrounding vegetation matrix is maximized (see Gonzalez et al., 2016). Once optimized, the CV workflow presented here should be easily implemented and provide time-efficient flying-fox colony size estimates relative to manual counts of thermal orthomosaics.

All four semi-automated classification methods tended to result in lower counts of flying-foxes in orthomosaics compared to manual point counts (Figure 4). The discrepancy between manual point counts and semi-automated counts for all methods may be due to misclassification of multiple close together flying-foxes as a single flying-fox, or failure to detect flying-foxes in warmer vegetation. Pixels are often misclassified if they lie on the boundary between two different land cover classes where pixels are a mix of reflected energy (Burke et al., 2019; Townshend et al., 2000), in this case heat from both flying-foxes and the background. This makes the definition of discrete boundaries between land classes difficult, such as in Supplementary Material 1.11, where bright vegetation (Bangalow palm, *Archontophoenix cunninghamiana*) was misclassified as flying-foxes in the top right corner of the orthomosaic. This issue was also described when discriminating glossy ibis (*Plegadis falcinellus*) from background in visual spectrum imagery using the Random Forest classifier (Afán et al., 2018). Furthermore, fewer flying-foxes were counted in 'Kareela 3', captured 3 h after sunrise, compared to 'Kareela 1' and 'Kareela 2' orthomosaics, captured earlier in the morning, by all human counters. Two human counters noted that 'Kareela 3' was more difficult to count due to a high amount

of bright vegetation in the orthomosaic because of solar glare, which made flying-foxes less distinguishable from the background, something that has been noted previously for sighting riverine rabbits (*Bunolagus monticularis*) in thermal imagery (Burke et al., 2019). Therefore, areas of bright vegetation may be misclassified by all semi-automated classification methods, so results from these semi-automated methods should be visually compared with the original orthomosaic to ensure their accuracy.

From pixel-based accuracy assessments, counts derived from thermal orthomosaics classified using the semi-automated classification methods were shown to have relatively high accuracies (average 84%). This suggests that the classification error lay in accurately quantifying and discriminating between groups of flying-foxes. However, using an object-based accuracy assessment method may have more accurately represented this issue and the count accuracy of each classified product (Terletzky & Ramsey, 2016). Nevertheless, in future studies improvements in sensor resolution should allow for improved discrimination between individual flying-foxes by semi-automated classification methods.

Conclusion

More accurate, precise and objective methods for monitoring the abundance of flying-foxes in a colony enhances the evidence base for the conservation and management of this globally threatened group of species (International Union for Conservation of Nature & Natural Resources, 2020). The drone-based thermal remote sensing method we demonstrate, enables reliable monitoring of population changes over time using an objective method, free from the biases associated with existing counting methods (Forsyth et al., 2006; Westcott & McKeown, 2004). If the method were implemented across whole species ranges, it would enable a more precise understanding of the spatial dynamics of flying-fox populations (Welbergen et al., 2020), the impacts of extreme weather events (Shilton et al., 2008; Welbergen et al., 2008), and the magnitude of flying-fox ecosystem services in a given location (van Toor et al., 2019). Understanding the drivers of flying-fox abundance and redistribution, and movements between roosts at the local and continental scales (Welbergen et al., 2020), will in turn enable researchers to develop predictive models for accurate and precise flying-fox population monitoring to inform conservation planning.

Acknowledgments

This research was supported by a Paddy Pallin Foundation-sponsored Australasian Bat Society grant to EDM, and an ARC Discovery Grant (DP170104272) to JAW. The authors thank Associate Professor Sebastian Pfautsch for generously loaning us the drone and thermal camera. We are also very grateful to the staff at Camellia Gardens, Bec Williams and Jaynia Sladek of Sutherland Shire Council, Andrew Jennings of Northern Beaches Council, Michael Ellison and Mitchell Clark of Campbelltown City Council, Amara Glynn of Centennial Parklands and Matthew Mo at NSW Department of Planning, Industry and Environment for assisting us with site access. Finally, we thank flying-fox counters Neroli Jackson, Roy Farman, Samantha Yabsley and Smitha Peter.

Conflict of Interest

Authors have no conflicts of interest to declare.

Author Contribution

All authors conceived the study. EDM performed the drone surveys, statistical analyses and led the writing of the manuscript. All authors contributed to drafts and gave final approval for publication.

Data Availability Statement

'Supplementary Material 1' is available as a pdf document. 'Supplementary Material 2' is stored in a zip file hosted on Figshare: http://doi.org/10.6084/m9.figshare.13138904.

References

Afán, I., Máñez, M. & Díaz-Delgado, R. (2018) Drone monitoring of breeding waterbird populations: the case of the glossy ibis. *Drones*, **2**(4), 42. https://doi.org/10.3390/drones2040042.

Agisoft LLC. (2019) *Agisoft Metashape user manual: professional edition, version 1.5*. Petersburg, Russia: Agisoft LLC.

Bowler, E., Fretwell, P.T., French, G. & Mackiewicz, M. (2020) Using deep learning to count albatrosses from space: assessing results in light of ground truth uncertainty. *Remote Sensing*, **12**(12), 2026. https://doi.org/10.3390/rs12122026.

Brooke, A.P. & Tschapka, M. (2002) Threats from overhunting to the flying fox, *Pteropus tonganus*, (Chiroptera: Pteropodidae) on Niue Island, South Pacific Ocean. *Biological Conservation*, **103**(3), 343–348. https://doi.org/10.1016/S0006-3207(01)00145-8.

Bureau of Meteorology. (2020) *Latest weather observations for the Sydney area* [Online]. Available at: http://www.bom.gov.au/nsw/observations/sydney.shtml?ref=hdr [Accessed 12 May 2020].

Burke, C., Rashman, M., Wich, S., Symons, A., Theron, C. & Longmore, S. (2019) Optimizing observing strategies for

monitoring animals using drone-mounted thermal infrared cameras. *International Journal of Remote Sensing*, **40**(2), 439–467. https://doi.org/10.1080/01431161.2018.1558372.

Bycroft, R., Leon, J.X. & Schoeman, D. (2019) Comparing random forests and convoluted neural networks for mapping ghost crab burrows using imagery from an unmanned aerial vehicle. *Estuarine Coastal and Shelf Science*, **224**, 84–93. https://doi.org/10.1016/j.ecss.2019.04.050.

Christie, K.S., Gilbert, S.L., Brown, C.L., Hatfield, M. & Hanson, L. (2016) Unmanned aircraft systems in wildlife research: current and future applications of a transformative technology. *Frontiers in Ecology and the Environment*, **14**(5), 241–251. https://doi.org/10.1002/fee.1281.

Cilulko, J., Janiszewski, P., Bogdaszewski, M. & Szczygielska, E. (2013) Infrared thermal imaging in studies of wild animals. *European Journal of Wildlife Research*, **59**(1), 17–23. https://doi.org/10.1007/s10344-012-0688-1.

Comaniciu, D. & Meer, P. (2002) Mean shift: A robust approach toward feature space analysis. *IEEE Transactions on Pattern Analysis and Machine Intelligence*, **24**(5), 603–619. https://doi.org/10.1109/34.1000236.

Commonwealth of Australia Department of Environment and Energy. (2019) *Flying-foxes and National Environment Law [Online]*. Available at: http://www.environment.gov.au/biodiversity/threatened/species/flying-fox-law [Accessed 23 June 2019].

Corcoran, E., Denman, S., Hanger, J., Wilson, B. & Hamilton, G. (2019) Automated detection of koalas using low-level aerial surveillance and machine learning. *Scientific Reports*, **9**(1), 3208. https://doi.org/10.1038/s41598-019-39917-5.

Cox, P.A., Elmqvist, T., Pierson, E.D. & Rainey, W.E. (1991) Flying foxes as strong interactors in South Pacific island ecosystems: a conservation hypothesis. *Conservation Biology*, **5**(4), 448–454. https://doi.org/10.1111/j.1523-1739.1991.tb00351.x.

Dell, A.I., Bender, J.A., Branson, K., Couzin, I.D., de Polavieja, G.G., Noldus, L.P.J.J. et al. (2014) Automated image-based tracking and its application in ecology. *Trends in Ecology & Evolution*, **29**(7), 417–428. https://doi.org/10.1016/j.tree.2014.05.004.

Dronova, I., Gong, P., Clinton, N.E., Wang, L., Fu, W., Qi, S. et al. (2012) Landscape analysis of wetland plant functional types: the effects of image segmentation scale, vegetation classes and classification methods. *Remote Sensing of Environment*, **127**, 357–369. https://doi.org/10.1016/j.rse.2012.09.018.

Drury, J.A., Nik, H., van Oppenraaij, R.H.F., Tang, A.-W., Turner, M.A. & Quenby, S. (2011) Endometrial cell counts in recurrent miscarriage: a comparison of counting methods. *Histopathology*, **59**(6), 1156–1162. https://doi.org/10.1111/j.1365-2559.2011.04046.x.

Dunstan, A., Robertson, K., Fitzpatrick, R., Pickford, J. & Meager, J. (2020) Use of unmanned aerial vehicles (UAVs) for mark-resight nesting population estimation of adult female green sea turtles at Raine Island. *PLoS One*, **15**(6), e0228524. https://doi.org/10.1371/journal.pone.0228524.

Eby, P., Richards, G., Collins, L. & Parry-Jones, K.A. (1999) The distribution, abundance and vulnerability to population reduction of a nomadic nectarivore, the grey-headed flying-fox *Pteropus poliocephalus* in New South Wales, during a period of resource concentration. *Australian Zoologist*, **31**(1), 240–253. https://doi.org/10.7882/az.1999.024.

Eisenbeiss, H. & Sauerbier, M. (2011) Investigation of UAV systems and flight modes for photogrammetric applications. *The Photogrammetric Record*, **26**(136), 400–421. https://doi.org/10.1111/j.1477-9730.2011.00657.x.

Environmental Systems Research Institute. (2020) *ArcGIS pro release 2.5.0*. Redlands, CA: Esri Inc.

Erwin, R.M. (1982) Observer variability in estimating numbers: an experiment. *Journal of Field Ornithology*, **53**(2), 159–167.

Forsyth, D.M., Scroggie, M.P. & McDonald-Madden, E. (2006) Accuracy and precision of grey-headed flying-fox (*Pteropus poliocephalus*) flyout counts. *Wildlife Research*, **33**(1), 57–65. https://doi.org/10.1071/WR05029.

Fox, J., Weisberg, S., Adler, D., Bates, D., Baud-Bovy, G., Ellison, S. et al. (2012) *Package 'car' [Online]*. Available at: http://cran-r.project.org/web/packages/car/car.pdf [Accessed 20 June 2020].

Francis, R.J., Lyons, M.B., Kingsford, R.T. & Brandis, K.J. (2020) Counting mixed breeding aggregations of animal species using drones: lessons from waterbirds on semi-automation. *Remote Sensing*, **12**(7), 1185. https://doi.org/10.3390/rs12071185.

Fujita, M.S. & Tuttle, M.D. (1991) Flying foxes (Chiroptera: Pteropodidae): threatened animals of key ecological and economic importance. *Conservation Biology*, **5**(4), 455–463. https://doi.org/10.1111/j.1523-1739.1991.tb00352.x.

Gibbs, J.P. (2000) Monitoring populations. In: Boitani, L. & Fuller, T.K. (Eds.) *Research techniques in animal ecology: controversies and consequences*. New York: Columbia University.

Goldsmith, B. (1991) *Monitoring for conservation and ecology*. London, United Kingdom: Chapman & Hall.

Gonzalez, L., Montes, G., Puig, E., Johnson, S., Mengersen, K. & Gaston, K. (2016) Unmanned aerial vehicles (UAVs) and artificial intelligence revolutionizing wildlife monitoring and conservation. *Sensors*, **16**(1), 97. https://doi.org/10.3390/s16010097.

Grishagin, I.V. (2015) Automatic cell counting with ImageJ. *Analytical Biochemistry*, **473**, 63–65. https://doi.org/10.1016/j.ab.2014.12.007.

Groom, G., Stjernholm, M., Nielsen, R.D., Fleetwood, A. & Petersen, I.K. (2013) Remote sensing image data and automated analysis to describe marine bird distributions and abundances. *Ecological Informatics*, **14**, 2–8. https://doi.org/10.1016/j.ecoinf.2012.12.001.

Guschanski, K., Vigilant, L., McNeilage, A., Gray, M., Kagoda, E. & Robbins, M.M. (2009) Counting elusive animals: comparing field and genetic census of the entire mountain gorilla population of Bwindi Impenetrable National Park, Uganda. *Biological Conservation*, **142**(2), 290–300. https://doi.org/10.1016/j.biocon.2008.10.024.

Hanger, J., de Villiers, D., Forbes, N., Nottidge, B., Beyer, H., Loader, J. et al. (2017) *Moreton Bay rail koala management program: final technical report for Queensland Department of Transport and Main Roads*. Toorbul: Endeavour Veterinary Ecology.

Harris, M.P. & Lloyd, C.S. (1977) Variations in counts of seabirds from photographs. *British Birds*, **70**(5), 200–205.

International Union for Conservation of Nature and Natural Resources. (2020) *The IUCN red list of threatened species [Online]*. Available at: http://www.iucnredlist.org/ [Accessed 22 May 2020].

Jiménez López, J. & Mulero-Pázmány, M. (2019) Drones for conservation in protected areas: present and future. *Drones*, **3**(1), 10. https://doi.org/10.3390/drones3010010.

Kays, R., Sheppard, J., McLean, K., Welch, C., Paunescu, C., Wang, V. et al. (2019) Hot monkey, cold reality: surveying rainforest canopy mammals using drone-mounted thermal infrared sensors. *International Journal of Remote Sensing*, **40**(2), 407–419. https://doi.org/10.1080/01431161.2018.1523580.

Lawrence, I. & Lin, K. (1989) A concordance correlation coefficient to evaluate reproducibility. *Biometrics*, **45**(1), 255–268. https://doi.org/10.2307/2532051.

Lhoest, S., Linchant, J., Quevauvillers, S., Vermeulen, C. & Lejeune, P. (2015) How many hippos (HOMHIP): algorithm for automatic counts of animals with infra-red thermal imagery from UAV. *The International Archives of the Photogrammetry, Remote Sensing and Spatial Information Sciences*, **XL-3/W3**, 355–362. https://doi.org/10.5194/isprsarchives-XL-3-W3-355-2015.

Manning, T., Edge, W.D. & Wolff, J.O. (1995) Evaluating population-size estimators: an empirical approach. *Journal of Mammalogy*, **76**(4), 1149–1158. https://doi.org/10.2307/1382606.

Margalida, A., Oro, D., Cortés-Avizanda, A., Heredia, R. & Donázar, J.A. (2011) Misleading population estimates: biases and consistency of visual surveys and matrix modelling in the endangered bearded vulture. *PLoS One*, **6**(10), e26784. https://doi.org/10.1371/journal.pone.0026784.

Markus, N. & Hall, L. (2004) Foraging behaviour of the black flying-fox (*Pteropus alecto*) in the urban landscape of Brisbane, Queensland. *Wildlife Research*, **31**(3), 345–355. https://doi.org/10.1071/WR01117.

Marsh, D.M. & Trenham, P.C. (2008) Current trends in plant and animal population monitoring. *Conservation Biology*, **22**(3), 647–655. https://doi.org/10.1111/j.1523-1739.2008.00927.x.

Meade, J., van der Ree, R., Stepanian, P.M., Westcott, D.A. & Welbergen, J.A. (2019) Using weather radar to monitor the number, timing and directions of flying-foxes emerging from their roosts. *Scientific Reports*, **9**(1), 10222. https://doi.org/10.1038/s41598-019-46549-2.

Mohd-Azlan, J., Zubaid, A. & Kunz, T.H. (2001) Distribution, relative abundance, and conservation status of the large flying fox, *Pteropus vampyrus*, in peninsular Malaysia: a preliminary assessment. *Acta Chiropterologica*, **3**(2), 149–162.

Mulero-Pázmány, M., Stolper, R., van Essen, L.D., Negro, J.J. & Sassen, T. (2014) Remotely piloted aircraft systems as a rhinoceros anti-poaching tool in Africa. *PLoS One*, **9**(1), e83873. https://doi.org/10.1371/journal.pone.0083873.

Old, J.M., Lin, S.H. & Franklin, M.J.M. (2019) Mapping out bare-nosed wombat (*Vombatus ursinus*) burrows with the use of a drone. *BMC Ecology*, **19**(1), 39. https://doi.org/10.1186/s12898-019-0257-5.

Phinn, S.R., Roelfsema, C.M. & Mumby, P.J. (2012) Multi-scale, object-based image analysis for mapping geomorphic and ecological zones on coral reefs. *International Journal of Remote Sensing*, **33**(12), 3768–3797. https://doi.org/10.1080/01431161.2011.633122.

Pinheiro, J., Bates, D., Debroy, S., Sarkar, D., Heisterkamp, S., van Willigen, B. et al. (2016) *Package 'nlme' [Online]*. Available at: https://cran.r-project.org/web/packages/nlme/nlme.pdf [Accessed 2 January 2020].

PIX4D. (2017) *Pix4Dmapper 4.1 user manual*. Lausanne, Switzerland: Pix4D SA.

R Core Team. (2018) *R: a language and environment for statistical computing*. Vienna, Austria: R Foundation for Statistical Computing.

Reddiex, B., Forsyth, D.M., McDonald-Madden, E., Einoder, L.D., Griffioen, P.A., Chick, R.R. et al. (2006) Control of pest mammals for biodiversity protection in Australia. I. Patterns of control and monitoring. *Wildlife Research*, **33**(8), 691–709. https://doi.org/10.1071/WR05102.

Reddy, S. & Dávalos, L.M. (2003) Geographical sampling bias and its implications for conservation priorities in Africa. *Journal of Biogeography*, **30**(11), 1719–1727. https://doi.org/10.1046/j.1365-2699.2003.00946.x.

Schindelin, J., Arganda-Carreras, I., Frise, E., Kaynig, V., Longair, M., Pietzsch, T. et al. (2012) Fiji: an open-source platform for biological-image analysis. *Nature Methods*, **9**(7), 676–682. https://doi.org/10.1038/nmeth.2019.

Seber, G.A.F. (1986) A review of estimating animal abundance. *Biometrics*, **42**(2), 267–292. https://doi.org/10.2307/2531049.

Seymour, A.C., Dale, J., Hammill, M., Halpin, P.N. & Johnston, D.W. (2017) Automated detection and enumeration of marine wildlife using unmanned aircraft systems (UAS) and thermal imagery. *Scientific Reports*, **7**, 45127. https://doi.org/10.1038/srep45127.

Shilton, L.A., Latch, P.J., McKeown, A., Pert, P. & Westcott, D.A. (2008) Landscape-scale redistribution of a highly mobile threatened species, *Pteropus conspicillatus* (Chiroptera, Pteropodidae), in response to Tropical Cyclone Larry. *Austral Ecology*, **33**(4), 549–561. https://doi.org/10.1111/j.1442-9993.2008.01910.x.

Signorell, A. (2016) *DescTools: tools for descriptive statistics*. [Online]. Available at: https://cran.r-project.org/web/packages/DescTools/index.html [Accessed 3 January 2020].

Spaan, D., Burke, C., McAree, O., Aureli, F., Rangel-Rivera, C.E., Hutschenreiter, A. et al. (2019) Thermal infrared imaging from drones offers a major advance for spider monkey surveys. *Drones*, **3**(2), 34. https://doi.org/10.3390/drones3020034.

Stapleton, S., Larue, M., Lecomte, N., Atkinson, S., Garshelis, D., Porter, C. et al. (2014) Polar bears from space: assessing satellite imagery as a tool to track Arctic wildlife. *PLoS One*, **9**(7), e101513. https://doi.org/10.1371/journal.pone.0101513.

Tabak, M.A., Norouzzadeh, M.S., Wolfson, D.W., Sweeney, S.J., Vercauteren, K.C., Snow, N.P. et al. (2019) Machine learning to classify animal species in camera trap images: applications in ecology. *Methods in Ecology and Evolution*, **10**(4), 585–590. https://doi.org/10.1111/2041-210X.13120.

Tait, J., Perotto-Baldivieso, H.L., McKeown, A. & Westcott, D.A. (2014) Are flying-foxes coming to town? Urbanisation of the spectacled flying-fox (*Pteropus conspicillatus*) in Australia. *PLoS One*, **9**(10), e109810. https://doi.org/10.1371/journal.pone.0109810.

Terletzky, P.A. & Ramsey, R.D. (2016) Comparison of three techniques to identify and count individual animals in aerial imagery. *Journal of Signal and Information Processing*, **7**(3), 123–135. https://doi.org/10.4236/jsip.2016.73013.

Timmiss L.A., Martin J.M., Murray N.J., Welbergen J.A., Westcott D., McKeown A. & Kingsford R.T. (2021) Threatened but not conserved: flying-fox roosting and foraging habitat in Australia. *Australian Journal of Zoology*, http://dx.doi.org/10.1071/zo20086.

Townshend, J.R.G., Huang, C., Kalluri, S.N.V., Defries, R.S., Liang, S. & Yang, K. (2000) Beware of per-pixel characterization of land cover. *International Journal of Remote Sensing*, **21**(4), 839–843. https://doi.org/10.1080/014311600210641.

Valletta, J.J., Torney, C., Kings, M., Thornton, A. & Madden, J. (2017) Applications of machine learning in animal behaviour studies. *Animal Behaviour*, **124**, 203–220. https://doi.org/10.1016/j.anbehav.2016.12.005.

van Toor, M.L., O'Mara, M.T., Abedi-Lartey, M., Wikelski, M., Fahr, J. & Dechmann, D.K.N. (2019) Linking colony size with quantitative estimates of ecosystem services of African fruit bats. *Current Biology*, **29**(7), R237–R238. https://doi.org/10.1016/j.cub.2019.02.033.

Wagner, J.L. (1981) Visibility and bias in avian foraging data. *The Condor*, **83**(3), 263–264. https://doi.org/10.2307/1367320.

Weinstein, B.G. (2018) A computer vision for animal ecology. *Journal of Animal Ecology*, **87**(3), 533–545. https://doi.org/10.1111/1365-2656.12780.

Welbergen, J.A., Klose, S.M., Markus, N. & Eby, P. (2008) Climate change and the effects of temperature extremes on Australian flying-foxes. *Proceedings of the Royal Society B: Biological Sciences*, **275**(1633), 419–425. https://doi.org/10.1098/rspb.2007.1385.

Welbergen, J.A., Meade, J., Field, H.E., Edson, D., McMichael, L., Shoo, L.P. et al. (2020) Extreme mobility of the world's largest flying mammals creates key challenges for management and conservation. *BMC Biology*, **18**(1), 101. https://doi.org/10.1186/s12915-020-00829-w.

Westcott, D.A. & McKeown, A. (2004) Observer error in exit counts of flying-foxes (*Pteropus* spp.). *Wildlife Research*, **31**(5), 551–558. https://doi.org/10.1071/WR03091.

Westcott, D.A., McKeown, A., Parry, H., Parsons, J., Jurdak, R., Kusy, B. et al. (2015) Implementation of the national flying-fox monitoring program. Australian Government, Rural Industries Research and Development Corporation.

Wich, S.A. & Koh, L.P. (2018) *Conservation drones: mapping and monitoring biodiversity*. Oxford, United Kingdom: Oxford University Press.

Woinarski, J. (2018) *A bat's end: the Christmas Island pipistrelle and extinction in Australia*. Clayton South, Australia: CSIRO Publishing.

Yang, Y. & Lee, X. (2019) Four-band thermal mosaicking: a new method to process infrared thermal imagery of urban landscapes from UAV flights. *Remote Sensing*, **11**(11), 1365. https://doi.org/10.3390/rs11111365.

Yang, Z., Wang, T., Skidmore, A.K., de Leeuw, J., Said, M.Y. & Freer, J. (2015) Spotting east African mammals in open savannah from space. *PLoS One*, **9**(12), e115989. https://doi.org/10.1371/journal.pone.0115989.

Supporting Information

Additional supporting information may be found online in the Supporting Information section at the end of the article.

Supplementary Material 1.1. Parameters used to generate thermal orthomosaics in Agisoft.

Supplementary Material 1.2. (A) Thermal image of flying-foxes roosting in a Eucalyptus sp. in the Centennial Park roost.

Supplementary Material 1.3. Manual point count results for orthomosaics generated from repeated surveys of the flying-fox colonies at Campbelltown, Kareela, Yarramundi, and Macquarie Fields.

Supplementary Material 1.4. Email sent out to the 4 participants in the study accessing between-counter variation in manual point counts of the number of flying-foxes in thermal orthomosaics.

Supplementary Material 1.5. Location, date of image acquisition, median air temperature at time of survey, average resolution, colony area, number of flying-foxes manually counted, and counted using the four semi-automated methods, for each orthomosaic to evaluate the accuracy of semi-automated methods.

Supplementary Material 1.6. Macro for implementing the Computer Vision classification workflow in Fiji 1.8.0_172 (Schindelin et al., 2012).

Supplementary Material 1.7. Machine learning classifier specifications for OBIA classification in ArcGIS Pro 2.5.0 (Environmental Systems Research Institute, 2020).

Supplementary Material 1.8. Flowchart outlining the steps taken to generate a semi-automated colony size estimate of the flying-fox colony at Yarramundi through OBIA and machine learning - implemented in ArcGIS Pro 2.5.0 (Environmental Systems Research Institute, 2020) and Fiji 1.8.0_172 (Schindelin et al., 2012).

Supplementary Material 1.9. Confusion matrix produced from an accuracy assessment of the Computer Vision classified drone-acquired thermal orthomosaic from the 3rd of September 2019 for the flying-fox colony at Yarramundi; (1) indicates commission error, (2) indicates omission error, and (3) indicates probability of detection.

Supplementary Material 1.10. (A) There was no significant effect of counter ID on manual point counts of flying-foxes in three thermal orthomosaics of the flying-fox colony at Kareela.

Supplementary Material 1.11. Completed accuracy assessment for the Random Forest classified product of the flying-fox colony at Camellia Gardens on the 22nd of October 2019, red points show pixels that were incorrectly classified using the Random Forest method, green points show correctly classified pixels.